

A dual-wavelength cladding-pumped Er-doped ZBLAN fiber laser emitting around 2.8 μm

Yuexuan Cai(蔡越轩), Dan Li(李丹), Guohao Fu(符国浩), Guanzhong Li(李冠中), Feng Yang(杨峰), Qirong Xiao(肖起榕), and Ping Yan(闫平)

Citation: Chin. Phys. B, 2026, 35 (**8**): 084204. DOI: 10.1088/1674-1056/ae1190
http://cpb.iphy.ac.cn; http://iopscience.iop.org/cpb

What follows is a list of articles you may be interested in

Comparison of cavity structures of 200 MHz repetition rate erbium-doped fiber lasers

Jiawei Liu(刘佳伟), Yuyao Zong(宗玉瑶), Yi Han(韩羿), and Shiying Cao(曹士英)
Chin. Phys. B, 2026, 35 (**6**): 064209. DOI: 10.1088/1674-1056/ae5f86

Generation of wavelength-tunable, bound-state and noise-like pulses in an all-polarization-maintaining laser ring cavity based on nonlinear polarization evolution

Yazhou Shi(石亚洲), Ze Li(李泽), and Zhiguo Lv(吕志国)
Chin. Phys. B, 2026, 35 (**5**): 054202. DOI: 10.1088/1674-1056/ae15f3

Simultaneous frequency stabilization of two 1550-nm lasers at single-photon level

Bo Yu(于波), Zhenqiang Yin(银振强), Weijie Ding(丁伟杰), Hui Yang(杨慧), and Weixin Liu(刘伟新)
Chin. Phys. B, 2026, 35 (**4**): 044208. DOI: 10.1088/1674-1056/ade072

Dissipative soliton operation in a mode-locked laser based on thulium-doped fiber

Wen-Yan Zhang(张文艳), Lei Zheng(郑磊), Tian Zhang(张添), Nan-Nan Liu(刘楠楠), Li-Jie Geng(耿利杰), Kun Yang(杨坤), and Li Zhan(詹黎)
Chin. Phys. B, 2026, 35 (**4**): 044201. DOI: 10.1088/1674-1056/ae063c

Full stabilization of eight-channel Yb-fiber coherent beam combining system delivering 1.18-kW, 1.18-mJ, 270-fs pulses

Zhuo Shi(史卓), Zhi-Hang Du(杜志航), Cheng-Bin Liang(梁成斌), Hong-Xiang Chang(常洪祥), Zi-Kai Dong(董自凯), Hong-Yu Guo(郭鸿宇), Can Li(李灿), Pu Zhou(周朴), Zhi-Yi Wei(魏志义), and Guo-Qing Chang(常国庆)
Chin. Phys. B, 2026, 35 (**2**): 024210. DOI: 10.1088/1674-1056/ae1952

A dual-wavelength cladding-pumped Er-doped ZBLAN fiber laser emitting around 2.8 μm

Yuexuan Cai(蔡越轩)[1,2,3], Dan Li(李丹)[1,2,3], Guohao Fu(符国浩)[1,2,3], Guanzhong Li(李冠中)[1,2,3], Feng Yang(杨峰)[4], Qirong Xiao(肖起榕)[1,2,3], and Ping Yan(闫平)[1,2,3,†]

[1] *Department of Precision Instrument, Tsinghua University, Beijing* 100084, *China*
[2] *State Key Laboratory of Precision Space-time Information Sensing Technology, Tsinghua University, Beijing* 100084, *China*
[3] *Key Laboratory of Photonics Control Technology of the Ministry of Education, Tsinghua University, Beijing* 100084, *China*
[4] *Southwest Institute of Technical Physics, Chengdu* 610041, *China*

(Received 13 August 2025; revised manuscript received 28 September 2025; accepted manuscript online 10 October 2025)

We demonstrate an Er-doped ZBLAN fiber laser emitting around 2.8 μm, with a distinctive dual-wavelength cladding-pumped approach. The laser was jointly cladding-pumped by a 1.568 μm fiber laser and a 1.68 μm laser diode, potentially lifting pump power constraints and achieving an enhanced efficiency. The corresponding simulation shows that the setup has better thermal management than other conventional pumping methods. At the maximum output power of 1.3 W, the optical efficiency was 19.1% relative to all absorbed pump and 42.5% relative to absorbed 1.68 μm pump after injection. With a higher pump power and further cavity optimization, the laser is expected to produce competitive powers. Moreover, optimal pump wavelength, dual-wavelength pump power relationship, and basic pump choice were also investigated, providing critical insights for high-power, high-efficiency and low-thermal-load 2.8 μm fiber laser systems.

Keywords: fiber laser, mid-infrared, dual-wavelength, cladding-pump

PACS: 42.55.Wd, 42.60.–v

DOI: 10.1088/1674-1056/ae1190 **CSTR:** 32038.14.CPB.ae1190

1. Introduction

Mid-infrared lasers operating around 2.8 μm have garnered interest due to their potential in critical technological domains, including materials processing, biomedical treatment, remote sensing, defense, and security.[1–4] Compared to other laser sources, fiber lasers exhibit advantages in high beam quality, excellent spectral characteristics, large power scalability, effective thermal management, and high system stability.[5–7] Due to powerful commercial 976 nm laser diodes and mature fluorozirconate-based active fibers, Er-doped ZBLAN fiber lasers have been effective sources to generate a high-power 2.8 μm laser relying on the $^4I_{11/2} \rightarrow {}^4I_{13/2}$ transition of Er^{3+} ions. However, the lifetime of the upper lasing level (7.9 ms) is shorter than that of the lower lasing level (9.9 ms), also known as the self-terminating effect, restraining laser generation and hindering efficiency improvement.

To facilitate population inversion between the upper and lower energy levels, there are two common strategies adopting 980 nm cladding-pumping: (1) utilizing the energy transfer up conversion (ETU1) effect in heavily doped fibers (> 5 mol%) to achieve $^4I_{13/2}$, $^4I_{13/2} \rightarrow {}^4I_{9/2}$, $^4I_{15/2}$ and (2) cascading 1.6 μm laser emission $^4I_{13/2} \rightarrow {}^4I_{15/2}$ in lightly doped fibers. For the first strategy, the output power of 41.6 W and 35.4 W was achieved,[8,9] while the low slope efficiency of 22.9% rendered thermal management challenging. The alternative one resulted in reduced 2.8 μm output efficiency due to the newly generated 1.6 μm laser emission, and made the fiber more susceptible to optical damage.[10,11]

As a matter of fact, using 1.68 μm pump-induced excited state absorption (ESA) transitions ($^4I_{13/2} \rightarrow {}^4I_{9/2}$) of Er^{3+} ions to deplete ions on the lower lasing level can not only recycle the population but also overcome the Stokes efficiency limit. Aydin *et al*. first addressed the process and utilized the 1614 nm laser within the cavity to provide the ESA process in the cascaded lasing structure, achieving a remarkable slope efficiency of nearly 50%.[12] Current research primarily focuses on two categories. (1) Dual-wavelength pumping: This scheme was first theoretically proposed for tellurite fibers,[13] where a 1.5 μm or 980 nm pump achieved population accumulation at $^4I_{13/2}$ via GSA1 or GSA2 respectively, followed by a 1.68 μm pump for ESA. Guo *et al*. implemented this scheme in ZBLAN fibers using 976 nm cladding-pump and 1.68 μm core-pump in a lightly doped fiber, achieving an output power of 1.2 W at 2.8 μm, with 33% overall optical efficiency.[14] (2) Single 1.68 μm pumping: It was theoretically proposed to use 1.68 μm core-pump drive GSA1 alongside ESA[5] and a 30.9% slope efficiency relative to absorbed pump power in heavily doped fibers could be acquired.[15] Li *et al*. achieved over 6 W, 2.8 μm output laser in a lightly doped fiber with a slope efficiency exceeding 50%.[16]

†Corresponding author. E-mail: pyan@mail.tsinghua.edu.cn

© 2026 Chinese Physical Society and IOP Publishing Ltd. All rights, including for text and data mining, AI training, and similar technologies, are reserved.

However, due to the extremely small absorption of GSA1 and insufficient absorption in lightly doped fibers, core-pumping of 1.68 μm seems necessary. It appears that the improvement of efficiency and pump injection capacity required for high power cannot be achieved simultaneously. In this paper, we report an advanced dual-wavelength cladding-pumped configuration for an Er-doped ZBLAN fiber laser emitting around 2.8 μm, adopting a 1.568 μm fiber laser as the basic pump through the GSA and a 1.68 μm laser diode for population inversion via the ESA. This pump scheme achieved an improvement in efficiency under dual-wavelength pumping while simultaneously lifting pump constraints potentially under cladding-pumping. Compared with the previous pumping scheme, the present design generates a markedly lower thermal load. The pump process is shown with energy levels and other relevant processes in Fig. 1. The optimization of pump parameters was also conducted in experiments.

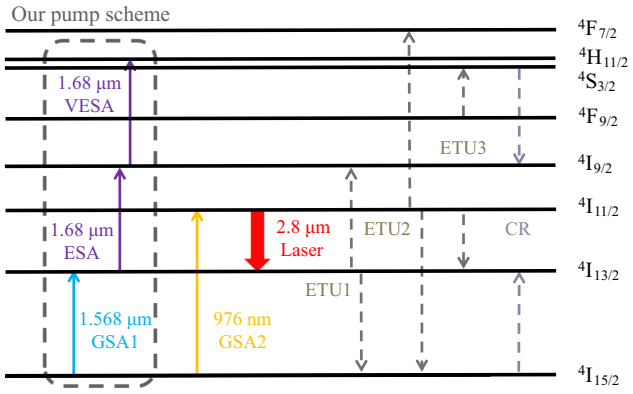


Fig. 1. Energy level diagram of Er^{3+} ions in ZBLAN fiber with the new pump scheme and relevant processes. VESA: virtual excited state absorption; CR: cross relaxation.

2. Experimental setup

The experimental setup of the laser is shown in Fig. 2. It had a backward-pumping configuration. The pump module consisted of a homemade FL, a 1.68 μm LD and a $(2+1)\times 1$ PSC. The FL employed an Er/Yb co-doped fiber as the active medium and operated at a central wavelength of 1.568 μm.[17] It was spliced to the 200/220 μm, NA-0.22 pump arm of the PSC. The 1.68 μm LD (supplied by Everbright Photonics) had a tunable central wavelength regulated through cooling temperature with a maximum output power of 40 W. It was delivered through a 200/220 μm, NA-0.22 silica fiber and spliced to the PSC's 30/250 μm, NA-0.065/0.46 signal fiber. Two pump sources were combined by the PSC and output through the 250 μm cladding of the PSC's signal fiber with a NA of 0.46. The gain medium was a 10-meter-long, 7 mol.% erbium-doped ZBLAN double-clad fiber (supplied by Le Verre Fluoré) with perpendicularly cleaved ends, having core/inner clad diameters of $15/240\times 260$ μm, and core/inner clad NA of 0.12/0.45. The pump was collimated by a fused silica aspheric lens L1 (diameter of 25.0 mm, focal length of 20.1 mm) and focused into the fiber cladding by a CaF_2 lens L2 (diameter of 25.4 mm, focal length of 25 mm) after transmitting through a dichroic mirror DM1 ($R>99\%$@2700–2900 nm, $T=97\%$@1550–1750 nm). The pump injection end utilized $\sim 4\%$ Fresnel feedback from the gain fiber facet to produce laser oscillation in the gain fiber. The opposite end was butt-coupled to a dichroic mirror DM2 ($R>99\%$@2700–2900 nm, $T=97\%$@1550–1750 nm) to provide high-reflection feedback. Hence, a laser cavity was formed within the gain fiber. The generated 2.8 μm laser was collimated by L2 and reflected out by the tilted DM1. Residual pump light was collimated and output via another fused silica aspheric lens L3 (diameter of 12 mm, focal length of 10.5 mm). The pump power after DM1 and the residual pump power after L3 were measured using a power meter PM1 (Ophir, 30A), while the reflected signal power from DM1 was quantified with a power meter PM2 (Thorlabs, S425C). The spectra of the pump and signal light were characterized through optical spectrum analyzers (Yokogawa AQ6370D and Yokogawa AQ6376) relatively. The pump coupling efficiency of 42% at 1.68 μm and 40% at 1.568 μm could be measured using the passive fiber with the same size. The actual absorbed pump power in the fiber was determined by subtracting the residual pump power measured after L3 from the total pump power coupled into the fiber.

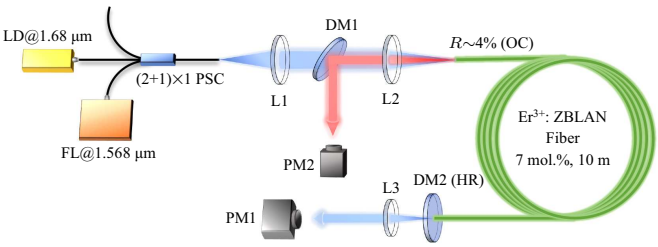


Fig. 2. Schematic diagram of the 2.8 μm laser system.

3. Results and discussion

3.1. Temperature and pump wavelength influence on the laser

We conducted the first comparative experiment with 1.68 μm pump wavelength shifted by cooling temperature. Initially, injecting 1.568 μm pump of 3.5 W resulted in a signal power of 0.516 W with a residual pump power of 0.059 W when the 1.68 μm pump was off, and an optical efficiency of 14.9% relative to the launched pump power, depending on the ETU1 process.[18] Subsequently, the 1.68 μm pump laser was introduced, and the cooling temperature of the LD exerted a measurable influence on both its emission wavelength and the system's overall output performance. The emission spectra were characterized as shown in Figs. 3(a)–3(c) at three

cooling temperatures (10 °C, 15 °C, and 20 °C) across different pump powers (referring to the 1.68 μm pump power coupled into the fiber). The center wavelengths red-shifted from 1674 nm to 1677 nm, 1680 nm, and 1684 nm with increasing pump power at 10 °C. At 15 °C, they were 1678 nm, 1681 nm, 1684 nm, and 1686 nm, and at 20 °C, they were 1680 nm, 1684 nm, 1687 nm, and 1690 nm. The output 2.8 μm signal power and 1.68 μm absorption efficiency as functions of the absorbed 1.68 μm pump power are plotted in Figs. 3(d)–3(f) at the three cooling temperatures. To the left of the dashed line, the signal power exhibited an increasing trend with absorbed pump power. At 10 °C, the maximum signal power reached 0.79 W with an optical efficiency of 49.4% relative to the absorbed 1.68 μm pump power (calculated as the ratio of the signal power minus 0.516 W to the absorbed 1.68 μm pump power). It should be mentioned that the change in residual 1.568 μm pump power of 0.059 W after the 1.68 μm pump injection was negligible. At 15 °C, these values were 0.87 W and 47%, and at 20 °C, they were 0.73 W and 41.4%. To the right of the dashed line, the signal power showed saturation because of thermal-induced deformation at the pump injection end led by low coupling efficiency (observed fiber-end temperatures exceeding 45 °C), which further degraded the coupling efficiency and wasted more pump. Under the three tested temperatures, the system exhibited the highest output power and optimal performance at 15 °C. While at 10 °C and 20 °C, premature saturation onset suggested partial diversion of pump into ETU at the expense of ESA in this wavelength regime, introducing additional heat besides the main thermal accumulation from low coupling efficiency and bringing earlier deformation. This demonstrated that pump wavelength at 15 °C in the region of 1678 nm–1681 nm enabled optimal ESA absorption efficiency while suppressing ion–ion interaction processes, consistent with direct spectroscopic measurements reported in Ref. [12].

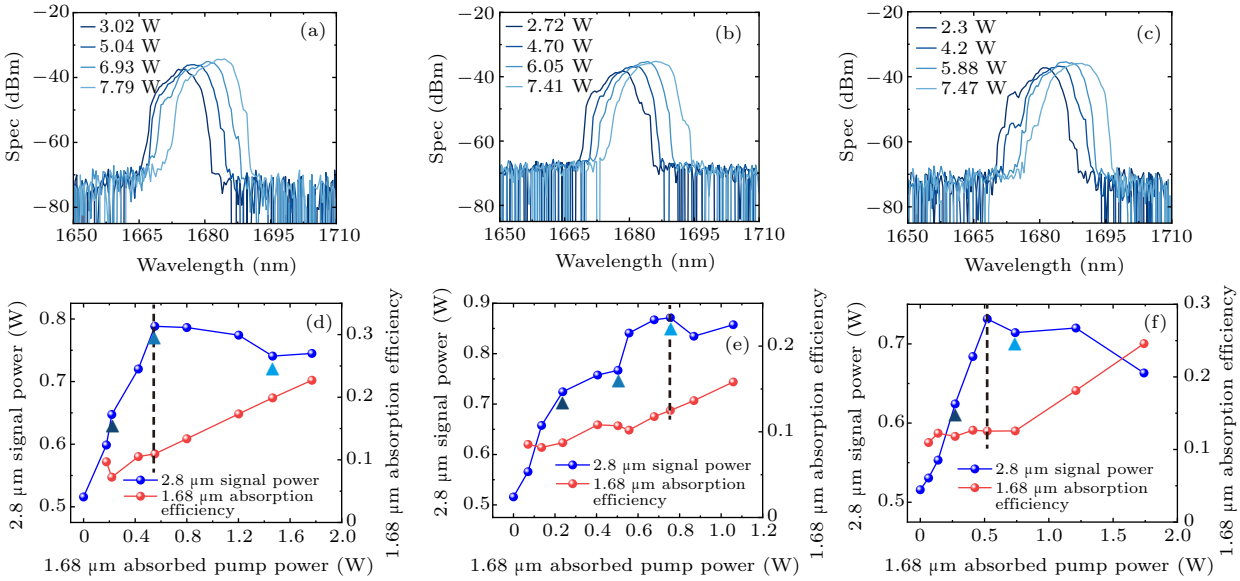


Fig. 3. Experimental results of the first experiment with a relatively low pump power of 1.568 μm. (a)–(c) Emission spectra of 1.68 μm LD at 10 °C, 15 °C and 20 °C respectively; (d–f) 2.8 μm signal power and 1.68 μm absorption efficiency versus absorbed 1.68 μm pump power at 10 °C, 15 °C and 20 °C respectively. The pump wavelengths are shown by triangles with the same color of spectra.

3.2. 2.8 μm laser operation with higher pump power

The second experiment was performed with more 1.568 μm pump power, maintaining the 1.68 μm LD cooling water temperature constant at 15 °C. Increasing the 1.568 μm pump power to 6.09 W produced a signal power of 0.96 W and a residual pump power of 0.093 W. Upon introducing the 1.68 μm pump, the pump absorption ratio peaked at 15% to the left of the dashed line, which was a measurable improvement over the results in Fig. 3(e). The system achieved a maximum output power of 1.3 W, corresponding to an overall optical efficiency of 19.1% relative to all absorbed pump power shown in Fig. 4(a). The optical efficiency reached 42.5% after 1.68 μm pump injection at maximum power operation (calculated as the ratio of the signal power minus 0.96 W to the absorbed 1.68 μm pump), verifying the efficiency improvement brought by the 1.68 μm pump. The inset illustrates the relationship between the signal and the 1.68 μm coupled pump, suggesting the need for system optimization to improve fiber absorption. Saturation effects persisted after increasing the pump power due to coupling efficiency degradation. The increase in the 1.568 μm pump raised the population of the $^4I_{13/2}$ energy level, which drove the absorption of the 1.68 μm pump. Spectral measurements were recorded at both the maximum signal power and the final signal power, centered at 2839.6 nm and 2810.2 nm, respectively, as depicted in Fig. 4(b). Spectral shift originated from longitudinal mode competition under the broadband reflectivity spectrum of DM1.

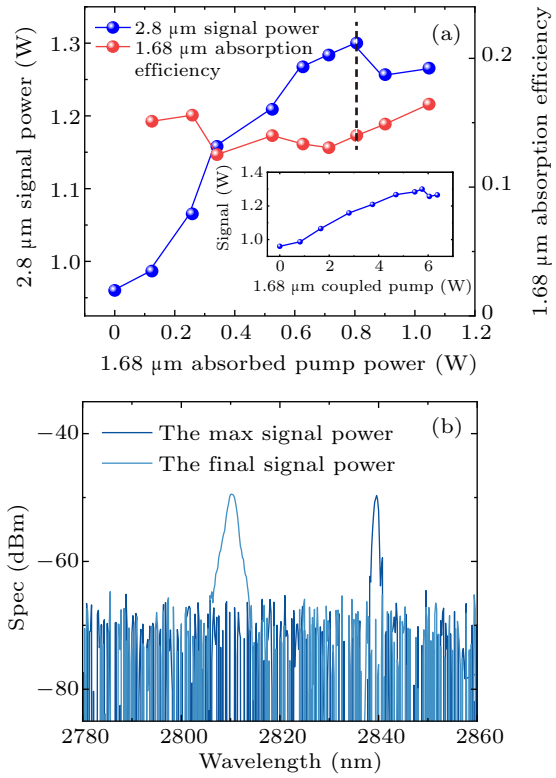


Fig. 4. Experimental results of the second experiment with a relatively high pump power of 1.568 μm. (a) 2.8 μm signal power, 1.68 μm absorption efficiency versus absorbed 1.68 μm pump power; inset: 2.8 μm signal power versus coupled 1.68 μm pump power; (b) spectral evolution of the max signal power and the final signal power point.

3.3. Basic pump choice and simulation for thermal load

To compare the performance between 1.568 μm and 976 nm as the basic pump, we conducted the third experiment by using the 976 nm pump as a basic pump source to achieve population accumulation in the $^4I_{13/2}$ level.[14] The 1.568 μm FL was replaced with a 976 nm LD. Still maintaining the 1.68 μm LD cooling temperature at 15 °C, we increased the 976 nm pump to 1.01 W, achieving 0.26 W signal output with 0.003 W residual pump. With the 1.68 μm pump turned on, the absorption ratio remained comparatively low due to the diminished contribution of the 976 nm pump to the left of the dashed line. The system reached a maximum output power of 0.38 W to the left, with an overall optical efficiency of 28.6% relative to all absorbed pump power and an optical efficiency after 1.68 μm pump injection of only 38.8% versus the absorbed 1.68 μm pump shown in Fig. 5(a). The limited efficiency might originate from stronger ETU2 under the 976 nm pump. Similar saturation behavior emerged on the right of the dashed line. Therefore, the 1.568 μm pump demonstrated a certain slope efficiency advantage as a basic pump source.

To evaluate the thermal performance of our pumping scheme under high power, the thermal load at the pump injection end of three cladding-pumping schemes was simulated: the 976 nm pumping scheme for 8 m fiber, the 976 nm +1.68 μm pumping scheme with the 976 nm basic pump of 30 W for 8 m fiber, and the 1.568 μm + 1.68 μm pumping scheme with the 1.568 μm basic pump of 30 W for 10 m fiber, neglecting external thermal factors like coupling. As shown in Fig. 5(b), the other two schemes exhibit more severe baseline thermal load and heat generation rate compared with our new pumping scheme under the same signal power due to stronger ETU1, ETU2, and insufficient population recycling, leading to increased non-radiative transitions. This fully demonstrates the thermal advantages of the new pumping scheme in high-power 2.8 μm fiber laser systems.

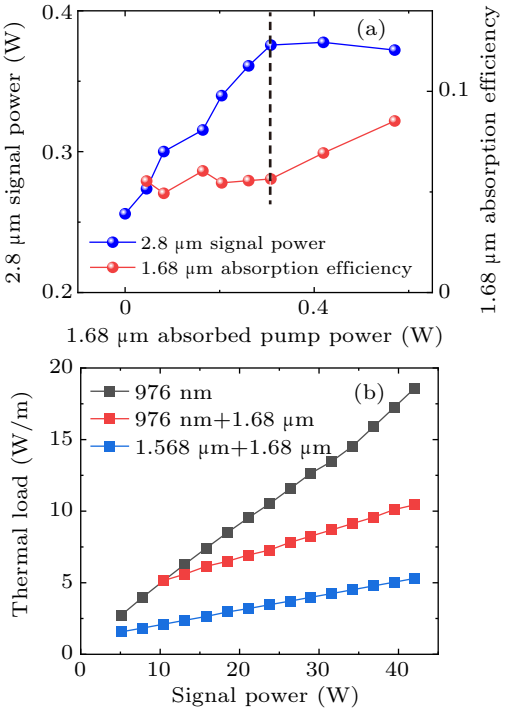


Fig. 5. Experimental results of the third experiment and simulation results for thermal load. (a) 2.8 μm signal power, 1.68 μm absorption efficiency versus absorbed 1.68 μm pump power with 976 nm LD as a basic pump source; (b) thermal load at the pump injection end of three pumping schemes.

3.4. Discussion

It is worth noting that the power saturation observed in the letter was predominantly from thermal distortion induced by low free-space coupling efficiency, rather than the dual-wavelength pumping scheme itself whose superior thermal management has been validated through simulations. The apparent increase in the 1.68 μm absorbed efficiency to the right of the dashed line confirms the saturation from coupling efficiency degradation, which reduces measured residual pump power and leads to an overestimation of calculated absorbed pump power, while actual absorbed power decreases. The saturation also differs from the VESA-induced quenching in Er-doped ZBLAN fiber during 3.5 μm lasing under dual-wavelength pumping.[19] Conversely, our pumping scheme itself exhibits enhanced resistance to quenching at a high power level with the reasons listed below: (1) The lifetime of the lower VESA level (8 μs) is far shorter than the one (177 μs) in Ref. [19], allowing most ions to undergo non-radiative

transitions towards the upper lasing level rather than VESA. (2) Cladding-pumping further suppresses VESA compared to core-pumping because of the much lower pump overlapping coefficient. The deformation-induced saturation effect can be mitigated by optimizing the PSC, notably through reducing the cladding diameter and NA of the output fiber, as the core diameter and NA of the 1.68 μm LD were much smaller than those after combination. Precise focal length matching of L1 and L2 can also improve pump coupling, as in our setup the image spot after collimation and focusing was 1.25 times larger than the object spot, exceeding the fiber cladding and thus limiting efficiency.

The above experimental results provide a verification of the feasibility of the proposed dual-wavelength cladding-pumping scheme. The introduction of the 1.68 μm pump in the novel pumping scheme has shown a substantial efficiency enhancement up to 42.5% versus absorbed pump power compared with the conventional 976 nm cladding-pump scheme. The dual-wavelength pumping scheme treats the $^4I_{13/2}$ level as a virtual ground state and gains an advantage in quantum efficiency. The adoption of the 1.68 μm LD and cladding pumping enables the possibility of achieving and injecting high pump power. These aspects highlight the potential of the proposed scheme for high-power implementation upon improvement of the coupling efficiency. Furthermore, the long-term stability of the laser is also important.[20] This pumping scheme enables long-term operation owing to its more uniform thermal distribution along the fiber and stable lower laser level population.

Compared with the 58.4% efficiency of core-pumped lightly-doped fibers,[16] our cladding-pumped heavily doped fiber shows slightly lower efficiency, mainly due to doping concentration rather than pump–core overlap. The reduced efficiency and weak absorption can be addressed by optimizing fiber parameters toward lightly doped and large core fibers. In heavily doped fibers, intense interaction like the ETU1 competes with the ESA, depleting the $^4I_{13/2}$ population, thereby reducing 1.68 μm absorption. Meanwhile, the ETU2 causes the loss of one photon energy through non-radiative transition, decreasing laser efficiency and increasing thermal generation. Overall, our simulation suggests that optimizing the fiber parameters to a doping concentration of 3 mol% and a core diameter of 35 μm can enhance the absorption coefficient of the 1.68 μm pump to 90%.

4. Conclusion

In summary, we demonstrated an Er-doped ZBLAN fiber laser emitting around 2.8 μm, with a distinctive dual-wavelength cladding-pumped approach. The system achieved a maximum output power of 1.3 W with an optical efficiency of 19.1% relative to all absorbed pump power and an optical efficiency of 42.5% relative to the absorbed 1.68 μm pump. Three experiments confirmed the optimal pump wavelength, investigated the dual-wavelength pump power relationship, and showed the advantage of the 1.568 μm as a basic pump. Despite being confined to lower power operation by coupling efficiency constraints, the efficiency improvement demonstrated in experiments, the potential pump power injection capability, and the thermal advantage verified through simulations provided critical insights for advancing high-power, high-efficiency, and low-thermal-load 2.8 μm fiber laser systems.

Acknowledgements

This work was supported by the National Natural Science Foundation of China (Grant Nos. 62475132 and 62122040), Beijing Natural Science Foundation (Grant No. L241021), the National Key Research and Development Program of China (Grant No. 2023YFB4604501), Tsinghua University (Department of Precision Instrument)–North Laser Research Institute Co., Ltd. Joint Research Center for Advanced Laser Technology (Grant No. 20244910194).

References

[1] Jackson S D 2012 *Nat. Photon.* **6** 423
[2] Tokita S, Murakami M, Shimizu S, Hashida M and Sakabe S 2009 *Opt. Lett.* **34** 3062
[3] Waynant R W, Ilev I K and Gannot I 2001 *Philos. Trans. Roy. Soc. London A.* **359** 635
[4] Zervas M N and Codemard C A 2014 *IEEE J. Sel. Topics Quantum Electron.* **20** 219
[5] Guo C Y, Lin J P, Tang Z Y, Li K Y, Tu L S, Wang J C, Liu X and Ruan S C 2022 *J. Lightwave Technol.* **40** 4397
[6] Jiang Y J, Su Y H, Gao J X, Zhou F, Cheng L Q, Pan K W, Sun B C, Shen L, Yang D X and Zhao J L 2025 *Chin. Phys. B* **34** 064203
[7] Wang X D, Geng X, Pan J Y, Sun M Q, Lu M X, Li K X and Li S W 2023 *Chin. Phys. B* **32** 024210
[8] Aydin Y O, Fortin V, Vallée R and Bernier M 2018 *Opt. Lett.* **43** 4542
[9] Goya K, Uehara H, Konishi D, Sahara R, Murakami M and Tokita S 2019 *Appl. Phys. Express* **12** 102007
[10] Jackson S D, Pollnau M and Li J F 2011 *IEEE J. Quantum Electron.* **47** 471
[11] Li J F, Wang L L, Luo H Y, Xie J T and Liu Y 2016 *IEEE Photon. Techno. Lett.* **28** 673
[12] Aydin Y O, Fortin V, Maes F, Jobin F, Jackson S D, Vallée R and Bernier M 2017 *Optica* **4** 235
[13] Anashkina E A, Andrianov A V, Dorofeev V V, Muravyev S V, Koptev M Y, Sorokin A A, Motorin S E, Koltashev V V, Galagan B I and Denker B I 2019 *Laser Phys. Lett.* **16** 025107
[14] Guo C Y, Shen P S, Ruan R S, Wang J C and Lue Q T 2023 *Infrared Phys. Technol.* **132** 104739
[15] Zhang J X, Wang R, Fu S J, Sheng Q, Xia W X, Zhang L, Shi W and Yao J Q 2022 *Opt. Lett.* **47** 3684
[16] Luo H Y, Shi J C, Chen J S, Wang Y Z, Li J F, Wu H and Liu Y 2024 *J. Lightwave Technol.* **42** 316
[17] Li G Z, Li D, Cai Y X, Fu G H, Yu W L, Li P, Xiao Q R, Gong M L and Yan P 2025 *J. Lightwave Technol.* **43** 4491
[18] Pattnaik R, Fromzel V, Zhang J and Dubinskii M 2020 *Laser Congress 2020 (ASSL, LAC)* AW5A.6
[19] Maes F, Fortin V, Bernier M and Vallée R 2017 *IEEE J. Quantum Electron.* **53** 1600208
[20] Chen S Y, Deng H Q, Zhang W R, Dai Y P, Wang T, Yu Q, Li C, Jiang M, Su R T, Wu J and Zhou P 2023 *Chin. Phys. B* **32** 074203